Title

A New Perspective and Design Principle for Halide Perovskites: Ionic Octahedron Network (ION)

Journal

Nano Letters, 21(12)

ISSN

1530-6984

Authors

Jin, Jianbo
Folgueras, Maria C
Gao, Mengyu
et al.

Publication Date

2021-06-23

DOI

10.1021/acs.nanolett.1c01897

Peer reviewed

A New Perspective and Design Principle for Halide Perovskites: Ionic Octahedron Network (ION)

Jianbo Jin[1,2], Maria C. Folgueras[2,3], Mengyu Gao[3,4], Sunmoon Yu[3], Sheena Louisia[1], Ye Zhang[1,4], Li Na Quan[4,†], Chubai Chen[1], Rui Zhang[2,5], Fabian Seeler[5], Kerstin Schierle-Arndt[2,5] ,and Peidong Yang[*,1,2,3,4,6]

1 Department of Chemistry, University of California, Berkeley, California 94720, United States

2 California Research Alliance (CARA), BASF Corporation, Berkeley, California 94720, United States

3 Department of Materials Science and Engineering, University of California, Berkeley, California 94720, United States

4 Materials Sciences Division, Lawrence Berkeley National Laboratory, Berkeley, California 94720, United States

5 BASF Corporation, Ludwigshafen am Rhein 67056, Germany

6 Kavli Energy NanoScience Institute, Berkeley, California 94720, United States

* Email: p_yang@berkeley.edu

KEYWORDS: octahedral building block, ionic octahedron network (ION), halide perovskites.

ABSTRACT:

The metal halide ionic octahedron, $[MX_6]$ (M = metal cation, X = halide anion), is considered to be the fundamental building block and functional unit of metal halide perovskites. By representing the metal halide ionic octahedron in halide perovskites as a super ion/atom, the halide perovskite can be described as an extended ionic octahedron network (ION) charge balanced by selected cations. This new perspective of halide perovskites based on ION enables the prediction of different packing and connectivity of the metal halide octahedra based on different solid-state lattices. In this work, a new halide perovskite $Cs_8Au_{3.5}In_{1.5}Cl_{23}$ was discovered based on a BaTiO3-lattice ION $\{[InCl_6][AuCl_5][Au/InCl_4]_3\}^{8-}$, which is assembled from three different ionic octahedra $[InCl_6]$, $[AuCl_6]$, and $[Au/InCl_6]$ and balanced by positively charged Cs cations. This success of this ION design concept in the discovery of $Cs_8Au_{3.5}In_{1.5}Cl_{23}$ opens up a new venue for the rational design of new halide perovskite materials.

Halide perovskites have been extensively studied as emergent semiconductor materials due to their remarkable optoelectronic properties,[1,2] and wide applications in solar cells[3–6], light-emitting diodes[7,8], photocatalysts[9], radiation detectors[10], etc. The halide perovskite family has the general formula of $APbX_3$ ($A = Cs^+$, Rb^+, etc., $X = Cl^-$, Br^-, I^-), which consists of a network of corner-sharing $[PbX_6]$ octahedra. The metal halide ionic octahedron is considered to be the fundamental building block and functional unit of halide perovskites[11], with dimension of 5-6 Å. Besides the lead halide perovskites, more complex structures appear when replacing Pb^{2+} with other metal cations. The design principle for many lead-free halide perovskites is generally based on charge balancing[12,13] (Figure S1). For example, when the divalent site (Pb^{2+}) is replaced with a monovalent and a trivalent cation (like Ag^+ and Bi^{3+}), the two cations will arrange in a rock-salt (NaCl) type structure, in the space group of $Fm\bar{3}m$.[14,15] Other structures form in perovskites with trivalent or quadrivalent metal cations coupled with vacancies, like $Cs_3Bi(III)_2X_9$[16] and $Cs_2Sn(IV)X_6$[17]. The emergence of lead-free halide perovskites provides more functional and environmentally friendly choices for various device applications.[18–20]

Inspired by the charge balancing design principle and the NaCl-type double halide perovskite, charge-ordered double perovskites, where the metal cations are mixed valence of the same element, including Au^+/Au^{3+}, Tl^+/Tl^{3+}, and In^+/In^{3+}, have also been investigated (Figure S2). [21–23] A pressure-induced semiconductor-to-metal phase transition of the charge-ordered $Cs_2In(I)In(III)Cl_6$ has also been spectroscopically observed in our previous work.[24] While many structures have been synthesized based on this design principle of charge balancing, recently we have turned our attention to the packing and interconnectivity of the $[MX_6]$ building block itself in order to discover new types of halide perovskites. To this end, we consider the ionic $[MX_6]$ octahedron as a super

ion/atom. Just as different atoms and ions can pack to form different crystal lattices, these ionic [MX_6] octahedra can in principle pack into different types of negatively charged, extended ionic octahedron networks (IONs), with and without corner sharing. Halide perovskite crystal structures are eventually formed when this negative charged ION is stabilized by counter cations (Scheme 1a). For example, the prototypical $CsPbX_3$ perovskites can be considered as a simple cubic lattice-based ION balanced by Cs cations, i.e., in the context of this ION concept, there is one [PbX_6] corner-shared octahedron and one Cs cation within the unit cell.

Scheme 1b summaries seven cubic IONs with different packing and interconnectivity. Vacancy-ordered double perovskites like Cs_2SnCl_6 can be viewed as having a face-centered-cubic-lattice ION, and there are 8 Cs cations and 4 [$SnCl_6$] octahedra within the unit cell. On the other hand, double halide perovskites like $Cs_2AgInCl_6$ correspond to a NaCl-lattice ION. There are again 8 Cs cations, and 4 [$AgCl_6$] and 4 [$InCl_6$] octahedra within one unit cell. The body-centered cubic-lattice ION (BCC) is not close packing, thus resulting in octahedron tilting in Cs_4PbBr_6 to stabilize the crystal structure (Figure S3).

With this general principle of the ionic octahedron network in mind, one could start to ask the following questions: what if we start to arrange these [MX_6] octahedra into lattices other than simple cubic, BCC, FCC or rock-salt? Will that lead to the discovery of new crystal structures for the halide perovskite family? For example, the CsCl-type ION could result in a structure with formula of $Cs_8M(I)M(III)Cl_{12}$, in the space group of $Pm\bar{3}m$ or slightly deviated because of octahedron rotation. ReO_3-type ION would result in a structure with the compositions $Cs_8M(I)M(III)_3X_{18}$ or $Cs_8M(IV)M(II)_3X_{18}$, in the space group of $Pm\bar{3}m$. In this particular case,

corner-shared [M(I/IV)X_6] and [M(III/II)X_6] octahedra would form a large ionic cage structure. Likewise, Perovskite-lattice ($BaTiO_3$-lattice) ION leads to a complex halide perovskite structure with the $Cs_8M(IV)M(III)M(III)_3X_{24}$ composition, in the space group of $Pm\bar{3}m$. Similarly, three octahedral units form a $BaTiO_3$-lattice ION according to the following formula: {[M(IV)X_6][M(III)X_6][M(III)X_6]$_3$} just like in BaTiO3 {ABX_3}, which is then balanced by the 8 Cs cations. After consideration of interconnectivity of the octahedral units, the final composition can be reduced to $Cs_8M(IV)M(III)M(III)_3X_{24}$. It is important to point out that so far in our discussion we have not considered the possible formation of halide vacancies in the structure, which is quite common in many inorganic halide perovskite lattices[25]. For example, it is conceivable that one can assemble a $BaTiO_3$ lattice-based ION using all trivalent cations by creating a halide vacancy in the structure, which would end up with a $Cs_8M(III)M(III)M(III)_3X_{23}$ stoichiometry. These halide perovskites predicted based on the CsCl, ReO_3, and $BaTiO_3$ lattice ION, however, have not been reported previously and yet to be confirmed experimentally. Here we detail our discovery of a new halide perovskite based on this predicted $BaTiO_3$ lattice ION. This packing and interconnecting of the sub-nano metal halide ionic octahedron building blocks represent a new line of thinking for the rational design of complex halide perovskite crystal structures.

We started with Au^{3+} and In^{3+} halide octahedra building blocks to test our idea of new design based on this ION principle, because they possess the same charge, similar radii, but different coordination behaviors (Figure S2). Simply by dissolving $HAuCl_4$, $InCl_3$, and CsCl into HCl solution, yellow octahedral shaped single crystals crystallized out of solution with slow cooling (Figure 1a, see Methods). Interestingly, the powder X-ray diffraction (PXRD) patterns show that

the resulting crystals have a simple cubic unit cell with a = 10.48 Å, doubled from the lattice parameter for $CsPbCl_3$ perovskites (Figure 1b). This observation is quite different from the $Cs_3M(III)_2X_9$ hexagonal structure with trivalent cations, and any other reported halide perovskites with two B-site cations in FCC (Figure S4). As seen in Figure 1b, there are diffraction peaks (labeled in red) in the PXRD patterns that should be systematically absent in the $Fm\bar{3}m$ space group but present in the simple cubic lattice. Energy-dispersive X-ray spectroscopy (EDS) confirms that the crystals have the composition of $Cs_8Au_{3.5}In_{1.5}Cl_{23}$ (Figure S5). To further characterize the oxidation states of the Au and In in the final crystals, X-ray photoelectron spectroscopy (XPS) is used to probe the Au 4f and In 3d core levels (Figure 1c,d) and the spectra confirms both elements exist dominantly as the trivalent oxidation state (Figure S6). During measurements, the surface and sub-surface Au^{3+} species can be reduced under X-ray irradiation, such that the shoulder peak which is attributed to the Au^{+} will increase in intensity as the exposure time increases. This is quite common for the Au^{3+} compounds[26], including $CsAu(III)Cl_4$ (Figure S7). In order to further confirm the oxidation states of the Au ions, X-ray absorption near edge structure (XANES) is also measured on the Au L_3-edge. For transition metals like Au, the L_3-edge XANES is dominated by a rising-edge[27]. Figure 1e shows exactly the same rising feature for both $Cs_8Au_{3.5}In_{1.5}Cl_{23}$ and the reference sample $CsAu(III)Cl_4$ in the Au L_3-edge XANES. The In K-edge XANES is also measured and is characterized by a strong white line peak feature corresponding to the transition of 2s core electrons into empty 5p states.[28] Figure 1f shows the white line feature of In in $Cs_8Au_{3.5}In_{1.5}Cl_{23}$ overlaps pretty well with the In^{3+} standard compound, $Cs_2In(III)Cl_5 \cdot H_2O$. The XANES confirms that both cations (Au and In) exist as +3 oxidation states in our crystals.

Single-crystal X-ray diffraction (SCXRD) is then used to resolve the crystal structure of the $Cs_8Au_{3.5}In_{1.5}Cl_{23}$. A simple cubic unit cell in space group of $Pm\bar{3}m$ was determined. The diffraction pattern also shows weak diffraction for (100), (110) and (210) peaks (Figure S8). The crystallographic table of $Cs_8Au_{3.5}In_{1.5}Cl_{23}$ (marked as $Cs_8Au_{3.5}In_{1.5}Cl_{23}$-Yellow) is listed in Table S2. The final crystal structure is determined as a new halide perovskite with a $BaTiO_3$-type ION in the formula of $Cs_8\{[InCl_6][AuCl_5][In/AuCl_4]_3$ (Figure 2a,b), as we have predicted and discussed in Scheme 1. A vacancy is formed at one of the Cl atom-sites to balance the overall charge. The calculated powder diffraction patterns from the determined crystal structure matches perfectly with the experimental PXRD results (Figure 1b). From the SCXRD, we can identify the metal species of each octahedron in the $BaTiO_3$-type (or more generally ABX_3-type) ION (Figure 2c). The super-"A" site is an isolated $[InCl_6]$ isotropic octahedron, the center metal is 100% occupancy of In, with In-Cl bond length of 2.530 Å. The super-"B" site is the $[AuCl_6]$ isotropic octahedron with only 5/6 occupation for the six bridging Cl atoms, the bond length of Au-bridging Cl is 2.392 Å. The super-"X" site is an elongated $[Au/InCl_6]$ metal halide octahedron. The metal occupancy is identified as 5/6 Au + 1/6 In from the electron density, which is in agreement with the occupancy of the bridging Cl. Bond length of $M\text{-}Cl_{5/6}$ (Bridging Cl) is 2.851 Å, while that of M-Cl is 2.308 Å. Bridging Cl atom links the "B" and "X" site octahedra. As a result, the $Cs_8Au_{3.5}In_{1.5}Cl_{23}$ is a new halide perovskite, with all ionic octahedra packed in the perovskite-type ION to yield the final stoichiometry $Cs_8\{[InCl_6][AuCl_5][In/AuCl_4]_3\}$, consistent with the prediction we made in Scheme 1. For the ABX_3-lattice ION, $[InCl_6][AuCl_5][In/AuCl_4]_3$ carries 8 negative charges and is balanced by the Cs cations within the lattice. This new structure represents the first example of rational design of new halide perovskites based on our concept of extended ION (Scheme 1).

While tuning the single crystal growth conditions, we discovered that when we use 6M HCl instead of 12M HCl, orange (rather than yellow) crystals are formed, with an extended absorption tail at longer wavelengths (Figure 3a, b). When we further apply heating (>95°C) during the synthesis, the resulting crystals are black. This could be attributed to the formation of Au(I) complexes during the synthesis. The $[Au(III)Cl_4]^-$ complex in acidic solution could decompose or be reduced into $[Au(I)Cl_2]^-$ under heating or irradiation.[29,30] As a result, there could be a small amount of this Au(I) complex formation in the solution, and its concentration can be influenced by heating and by the HCl concentration. The introduction of Au(I) into this particular ionic network could result in the change of the electronic structure, and consequently their optical properties.

With this hypothesis on the role of mixed-valency in this extended ionic network, controlled reduction experiments were carried out by adding small amounts of reducing agents such as L-ascorbic acid (AA) before the crystallization of the crystals. Figure 3a shows that we can grow different colored crystals with the addition of AA. Figure 3b shows systematic red shifting of the absorption across theses crystals and indicates bandgap narrowing with an increasing amount of reduced Au(I). The results confirmed that introduction of the Au(I) dopants would reduce the absorption bandgap of the $Cs_8Au_{3.5}In_{1.5}Cl_{23}$ new halide perovskites from 2.37eV to 1.43eV, a value that is quite comparable with that of $Cs_2Au(I)Au(III)Cl_6$.[31] The Au(I) dopant concentration produced with different molar ratios of AA can be estimated from the decrease in intensity of the characteristic absorption peak of $[AuCl_4]^-$ at 313 nm.[32] This analysis suggests that less than 3% of the $[AuCl_4]^-$ will be reduced with AA when the molar ratio of AA is less than 5% (Figure S9). XANES on the Au L_3 edge also indicates only negligible Au(I) exists in the doped crystals (Figure 3c). Both inductively coupled plasma atomic emission spectroscopy (ICP-AES) and mass

spectroscopy (ICP-MS) measurements confirmed no significant changes in Au:In ratio upon Au(I) doping (Table S1). PXRD shows no changes in the simple cubic structure across the various crystals and only a slight modification in lattice parameter to 10.49 Å with Au(I) dopants (Figure 3d). SCXRD measurements were also collected on the black crystals (Table S2, $Cs_8Au_{3.5}In_{1.5}Cl_{23}$-Black) and showed the structure is still essentially the same overall structure as $Cs_8\{[InCl_6][AuCl_5][In/AuCl_4]_3$. Raman measurements (Figure 3e) show the emergence of new vibrational modes with the presence of Au(I) dopants in the crystal structure, as well as second harmonic features which are also observed in $Cs_2Au(I)Au(III)Cl_6$ halide perovskites.[34] This set of experiments suggest that once we establish the overall ionic octahedron network, $BaTiO_3$-lattice in this case, it is possible to further modify the optical and electronic properties by introducing mixed-valency within this interconnected network. Further detailed studies including electronic structure calculations of these new halide perovskites are in progress.

In conclusion, we propose here a new perspective and design principle of halide perovskites based on a collection of extended ionic octahedron network (ION) balanced by counter cations. Using this new design concept, we have discovered a new halide perovskite structure, $Cs_8Au_{3.5}In_{1.5}Cl_{23}$, or $Cs_8\{[InCl_6][AuCl_5][In/AuCl_4]_3\}$, which can be considered as a $BaTiO_3$-type ION charge balanced with Cs cations. This is the first reported example of halide perovskites predicted based on this ionic octahedron network concept. With this powerful ION design principle, one can further replace one of the trivalent cations with a quadrivalent cation, to achieve the $Cs_8M(IV)M(III)M(III)_3X_{24}$ halide perovskites with the $BaTiO_3$-type ION as we have discussed in Scheme 1. There are potentially more new perovskite structures to be discovered based on this ION design principle, including new halide perovskite structures based on CsCl-type and ReO_3-

type ION, e.g., $Cs_8M(I)M(III)X_{12}$, $Cs_8M(I)M(III)_3X_{18}$ or $Cs_8M(IV)M(II)_3X_{18}$. We now have an enormous synthetic space to design and synthesize new halide perovskite crystal structures, considering that we can explore many different ways of packing and interconnectivity of the octahedral units with different halide ions and balancing counter cations. Additionally, introducing mixed-valency into this overall extended ION network design enables further structural and electronic tunability.

ASSOCIATED CONTENT

Supporting Information

The Supporting Information is available free of charge on the ACS Publications website at DOI:…

Description of experimental details and additional characterization data. Figures showing SEM images, EDS results, XPS spectra, tables showing single-crystal XRD crystallographic results, including Figure S1-S9, Table S1-S2. (PDF)

Crystal Structure of $Cs_8Au_{3.5}In_{1.5}Cl_{23}$-Yellow (CIF)

Checkcif Report of $Cs_8Au_{3.5}In_{1.5}Cl_{23}$-Yellow (PDF)

Crystal Structure of $Cs_8Au_{3.5}In_{1.5}Cl_{23}$-Black (CIF)

Checkcif Report of $Cs_8Au_{3.5}In_{1.5}Cl_{23}$-Black (PDF)

Accession Code:

The crystallographic information file (CIF) has also been deposited in the Inorganic Crystal Structure Database under reference number CSD 2082755 and 2082756. These data can be obtained free of charge via https://www.ccdc.cam.ac.uk/structures/, or by emailing data_request@ccdc.cam.ac.uk.

AUTHOR INFORMATION

Corresponding Author

*Email: p_yang@berkeley.edu

ORCID

Jianbo Jin: 0000-0002-9054-7960

Maria C. Folgueras: 0000-0001-6502-7616

Mengyu Gao: 0000-0003-1385-7364

Sheena Louisia, 0000-0002-2175-6769

Sunmoon Yu: 0000-0001-7250-9365

Ye Zhang: 0000-0001-5953-2173

Li Na Quan: 0000-0001-9301-3764

Chubai Chen: 0000-0003-2513-2707

Peidong Yang: 0000-0003-4799-1684

Present Addresses

† Li Na Quan: Department of Chemistry, Virginia Polytechnic Institute and State University, Blacksburg, VA 24061

Author Contributions

The manuscript was written with contributions of all authors. All authors have given approval to the final version of the manuscript.

Notes

The authors declare no competing financial interest.

During the preparation of this manuscript, we found a similar structure has been reported by K. P. Lindquisint *et al.*, in *J. Am. Chem. Soc*, DOI: 10.1021/jacs.1c01624.

ACKNOWLEDGMENT

The authors thank Ms. Xiaokun Pei, Dr. Jia Lin, Dr. Hong Chen, and Dr. Nils-Olof Born for helpful discussions. This work was financially supported by the BASF CARA program (No. 87456997). Single-crystal X-ray Diffraction studies were performed at the UC Berkeley College of Chemistry X-ray Crystallography (CheXray) and beamline 12.2.1 at the Advanced Light Source (ALS) at Lawrence Berkeley National Lab (LBNL). We thank Dr. Nick Settineri at UC Berkeley and Dr. Simon Teat at ALS for their helps in SCXRD collection. We thank Dr. Kevin H. Stone for Synchrotron Powder XRD data collection at beamline 2-1 of Stanford Synchrotron Radiation Lightsource (SSRL), SLAC National Accelerator Laboratory (DE-AC02-76SF00515). We thank Dr. Lu Ma and Dr. Steven Ehrlich for XAS data at beamline 7-BM of the National Synchrotron Light Source II (NSLS-II), Brookhaven National Laboratory (BNL) (DE-SC0012704). We thank Dr. Austin M. Chole for ICP-MS sample preparation and data collection at the UC Davis Interdisciplinary Center for Plasma Mass Spectrometry (UCD/ICPMS). Ultralow-frequency Raman spectroscopy was performed at the Stanford Nano Shared Facilities (SNSF), supported by the National Science Foundation (ECCS-1542152). J.J. and Y.Z. acknowledge the fellowship support from Suzhou Industrial Park. S.Y. acknowledges support from Samsung Scholarship.

REFERENCES

(1) Manser, J. S.; Christians, J. A.; Kamat, P. v. Intriguing Optoelectronic Properties of Metal Halide Perovskites. *Chemical Reviews* **2016**, *116* (21), 12956–13008. https://doi.org/10.1021/acs.chemrev.6b00136.

(2) Kovalenko, M. v; Protesescu, L.; Bodnarchuk, M. I. Properties and Potential Optoelectronic Applications of Lead Halide Perovskite Nanocrystals. *Science* **2017**, *358* (6364), 745. https://doi.org/10.1126/science.aam7093.

(3) Lee, M. M.; Teuscher, J.; Miyasaka, T.; Murakami, T. N.; Snaith, H. J. Efficient Hybrid Solar Cells Based on Meso-Superstructured Organometal Halide Perovskites. *Science* **2012**, *338* (6107), 643. https://doi.org/10.1126/science.1228604.

(4) Burschka, J.; Pellet, N.; Moon, S.-J.; Humphry-Baker, R.; Gao, P.; Nazeeruddin, M. K.; Grätzel, M. Sequential Deposition as a Route to High-Performance Perovskite-Sensitized Solar Cells. *Nature* **2013**, *499* (7458), 316–319. https://doi.org/10.1038/nature12340.

(5) Green, M. A.; Ho-Baillie, A.; Snaith, H. J. The Emergence of Perovskite Solar Cells. *Nature Photonics* **2014**, *8* (7), 506–514. https://doi.org/10.1038/nphoton.2014.134.

(6) Jeon, N. J.; Noh, J. H.; Yang, W. S.; Kim, Y. C.; Ryu, S.; Seo, J.; Seok, S. il. Compositional Engineering of Perovskite Materials for High-Performance Solar Cells. *Nature* **2015**, *517* (7535), 476–480. https://doi.org/10.1038/nature14133.

(7) Tan, Z.-K.; Moghaddam, R. S.; Lai, M. L.; Docampo, P.; Higler, R.; Deschler, F.; Price, M.; Sadhanala, A.; Pazos, L. M.; Credgington, D.; Hanusch, F.; Bein, T.; Snaith, H. J.; Friend, R. H. Bright Light-Emitting Diodes Based on Organometal Halide Perovskite. *Nature Nanotechnology* **2014**, *9* (9), 687–692. https://doi.org/10.1038/nnano.2014.149.

(8) Chen, H.; Lin, J.; Kang, J.; Kong, Q.; Lu, D.; Kang, J.; Lai, M.; Quan, L. N.; Lin, Z.; Jin, J.; Wang, L.; Toney, M. F.; Yang, P. Structural and Spectral Dynamics of Single-Crystalline Ruddlesden-Popper Phase Halide Perovskite Blue Light-Emitting Diodes. *Science Advances* **2020**, *6* (4), eaay4045. https://doi.org/10.1126/sciadv.aay4045.

(9) Huang, H.; Pradhan, B.; Hofkens, J.; Roeffaers, M. B. J.; Steele, J. A. Solar-Driven Metal Halide Perovskite Photocatalysis: Design, Stability, and Performance. *ACS Energy Letters* **2020**, *5* (4), 1107–1123. https://doi.org/10.1021/acsenergylett.0c00058.

(10) Chen, Q.; Wu, J.; Ou, X.; Huang, B.; Almutlaq, J.; Zhumekenov, A. A.; Guan, X.; Han, S.; Liang, L.; Yi, Z.; Li, J.; Xie, X.; Wang, Y.; Li, Y.; Fan, D.; Teh, D. B. L.; All, A. H.; Mohammed, O. F.; Bakr, O. M.; Wu, T.; Bettinelli, M.; Yang, H.; Huang, W.; Liu, X. All-Inorganic Perovskite Nanocrystal Scintillators. *Nature* **2018**, *561* (7721), 88–93. https://doi.org/10.1038/s41586-018-0451-1.

(11) Lin, H.; Zhou, C.; Tian, Y.; Siegrist, T.; Ma, B. Low-Dimensional Organometal Halide Perovskites. *ACS Energy Letters* **2018**, *3* (1), 54–62. https://doi.org/10.1021/acsenergylett.7b00926.

(12) Zhao, X.-G.; Yang, D.; Ren, J.-C.; Sun, Y.; Xiao, Z.; Zhang, L. Rational Design of Halide Double Perovskites for Optoelectronic Applications. *Joule* **2018**, *2* (9), 1662–1673. https://doi.org/https://doi.org/10.1016/j.joule.2018.06.017.

(13) Xiao, Z.; Song, Z.; Yan, Y. From Lead Halide Perovskites to Lead-Free Metal Halide Perovskites and Perovskite Derivatives. *Advanced Materials* **2019**, *31* (47), 1803792. https://doi.org/https://doi.org/10.1002/adma.201803792.

(14) Slavney, A. H.; Hu, T.; Lindenberg, A. M.; Karunadasa, H. I. A Bismuth-Halide Double Perovskite with Long Carrier Recombination Lifetime for Photovoltaic Applications. *Journal of the American Chemical Society* **2016**, *138* (7), 2138–2141. https://doi.org/10.1021/jacs.5b13294.

(15) McClure, E. T.; Ball, M. R.; Windl, W.; Woodward, P. M. Cs_2AgBiX_6 (X = Br, Cl): New Visible Light Absorbing, Lead-Free Halide Perovskite Semiconductors. *Chemistry of Materials* **2016**, *28* (5), 1348–1354. https://doi.org/10.1021/acs.chemmater.5b04231.

(16) Bass, K. K.; Estergreen, L.; Savory, C. N.; Buckeridge, J.; Scanlon, D. O.; Djurovich, P. I.; Bradforth, S. E.; Thompson, M. E.; Melot, B. C. Vibronic Structure in Room Temperature Photoluminescence of the Halide Perovskite Cs3Bi2Br9. *Inorganic Chemistry* **2017**, *56* (1), 42–45. https://doi.org/10.1021/acs.inorgchem.6b01571.

(17) Lee, B.; Stoumpos, C. C.; Zhou, N.; Hao, F.; Malliakas, C.; Yeh, C.-Y.; Marks, T. J.; Kanatzidis, M. G.; Chang, R. P. H. Air-Stable Molecular Semiconducting Iodosalts for Solar Cell Applications: Cs_2SnI_6 as a Hole Conductor. *Journal of the American Chemical Society* **2014**, *136* (43), 15379–15385. https://doi.org/10.1021/ja508464w.

(18) Chung, I.; Lee, B.; He, J.; Chang, R. P. H.; Kanatzidis, M. G. All-Solid-State Dye-Sensitized Solar Cells with High Efficiency. *Nature* **2012**, *485* (7399), 486–489. https://doi.org/10.1038/nature11067.

(19) Luo, J.; Wang, X.; Li, S.; Liu, J.; Guo, Y.; Niu, G.; Yao, L.; Fu, Y.; Gao, L.; Dong, Q.; Zhao, C.; Leng, M.; Ma, F.; Liang, W.; Wang, L.; Jin, S.; Han, J.; Zhang, L.; Etheridge, J.; Wang, J.; Yan, Y.; Sargent, E. H.; Tang, J. Efficient and Stable Emission of Warm-White Light from Lead-Free Halide Double Perovskites. *Nature* **2018**, *563* (7732), 541–545. https://doi.org/10.1038/s41586-018-0691-0.

(20) Huang, J.; Lei, T.; Siron, M.; Zhang, Y.; Yu, S.; Seeler, F.; Dehestani, A.; Quan, L. N.; Schierle-Arndt, K.; Yang, P. Lead-Free Cesium Europium Halide Perovskite Nanocrystals. *Nano Letters* **2020**, *20* (5), 3734–3739. https://doi.org/10.1021/acs.nanolett.0c00692.

(21) Kojima, N.; Hasegawa, M.; Kitagawa, H.; Kikegawa, T.; Shimomura, O. P-T Phase Diagram and Gold Valence State of the Perovskite-Type Mixed-Valence Compounds $Cs_2Au_2X_6$ (X = Cl, Br, and I) under High Pressures. *Journal of the American Chemical Society* **1994**, *116* (25), 11368–11374. https://doi.org/10.1021/ja00104a016.

(22) Wang, S.; Hirai, S.; Shapiro, M. C.; Riggs, S. C.; Geballe, T. H.; Mao, W. L.; Fisher, I. R. Pressure-Induced Symmetry Breaking in Tetragonal $CsAuI_3$. *Physical Review B* **2013**, *87* (5), 54104. https://doi.org/10.1103/PhysRevB.87.054104.

(23) Retuerto, M.; Emge, T.; Hadermann, J.; Stephens, P. W.; Li, M. R.; Yin, Z. P.; Croft, M.; Ignatov, A.; Zhang, S. J.; Yuan, Z.; Jin, C.; Simonson, J. W.; Aronson, M. C.; Pan, A.; Basov, D. N.; Kotliar, G.; Greenblatt, M. Synthesis and Properties of Charge-Ordered Thallium Halide Perovskites, $CsTl^{+}_{0.5}Tl^{3+}_{0.5}X_3$ (X = F or Cl): Theoretical Precursors for Superconductivity? *Chemistry of Materials* **2013**, *25* (20), 4071–4079. https://doi.org/10.1021/cm402423x.

(24) Lin, J.; Chen, H.; Gao, Y.; Cai, Y.; Jin, J.; Etman, A. S.; Kang, J.; Lei, T.; Lin, Z.; Folgueras, M. C.; Quan, L. N.; Kong, Q.; Sherburne, M.; Asta, M.; Sun, J.; Toney, M. F.; Wu, J.; Yang, P. Pressure-Induced Semiconductor-to-Metal Phase Transition of a Charge-Ordered Indium Halide Perovskite. *Proceedings of the National Academy of Sciences* **2019**, *116* (47), 23404. https://doi.org/10.1073/pnas.1907576116.

(25) Li, C.; Guerrero, A.; Huettner, S.; Bisquert, J. Unravelling the Role of Vacancies in Lead Halide Perovskite through Electrical Switching of Photoluminescence. *Nature Communications* **2018**, *9* (1), 5113. https://doi.org/10.1038/s41467-018-07571-6.

(26) Crist, B. Vincent. Handbooks of Monochromatic XPS Spectra: Volume 2: Commercially Pure Binary Oxides. Published by *XPS International LLC, California,* **2004**.

(27) Tanino, H.; Takahashi, K. Valence Study of Au in $Cs_2Au(I)Au(III)Cl_6$ and $Cs_2Ag(I)Au(III)X_6$(X= Cl, Br) by X-Ray Absorption Spectra at the Au L3 Edge. *Solid State Communications* **1986**, *59* (12), 825–827. https://doi.org/https://doi.org/10.1016/0038-1098(86)90637-X.

(28) Tan, X.; Stephens, P. W.; Hendrickx, M.; Hadermann, J.; Segre, C. U.; Croft, M.; Kang, C.-J.; Deng, Z.; Lapidus, S. H.; Kim, S. W.; Jin, C.; Kotliar, G.; Greenblatt, M. Tetragonal $Cs_{1.17}In_{0.81}Cl_3$: A Charge-Ordered Indium Halide Perovskite Derivative. *Chemistry of Materials* **2019**, *31* (6), 1981–1989. https://doi.org/10.1021/acs.chemmater.8b04771.

(29) Gammons, C. H.; Yu, Y.; Williams-Jones, A. E. The Disproportionation of Gold(I) Chloride Complexes at 25 to 200°C. *Geochimica et Cosmochimica Acta* **1997**, *61* (10), 1971–1983. https://doi.org/https://doi.org/10.1016/S0016-7037(97)00060-4.

(30) Guo, Y.; Zhang, L.; Zhou, K.; Shen, Y.; Zhang, Q.; Gu, C. Selective Gold Recovery by Carbon Nitride through Photoreduction. *Journal of Materials Chemistry A* **2014**, *2* (46), 19594–19597. https://doi.org/10.1039/C4TA04400B.

(31) Bajorowicz, B.; Mikolajczyk, A.; Pinto, H. P.; Miodyńska, M.; Lisowski, W.; Klimczuk, T.; Kaplan-Ashiri, I.; Kazes, M.; Oron, D.; Zaleska-Medynska, A. Integrated Experimental and Theoretical Approach for Efficient Design and Synthesis of Gold-Based Double Halide Perovskites. *The Journal of Physical Chemistry C* **2020**, *124* (49), 26769–26779. https://doi.org/10.1021/acs.jpcc.0c07782.

(32) Đurović, M. D.; Puchta, R.; Bugarčić, Ž. D.; van Eldik, R. Studies on the Reactions of $[AuCl_4]^-$ with Different Nucleophiles in Aqueous Solution. *Dalton Transactions* **2014**, *43* (23), 8620–8632. https://doi.org/10.1039/C4DT00247D.

(33) Slavney, A. H.; Leppert, L.; Bartesaghi, D.; Gold-Parker, A.; Toney, M. F.; Savenije, T. J.; Neaton, J. B.; Karunadasa, H. I. Defect-Induced Band-Edge Reconstruction of a Bismuth-Halide Double Perovskite for Visible-Light Absorption. *Journal of the American Chemical Society* **2017**, *139* (14), 5015–5018. https://doi.org/10.1021/jacs.7b01629.

(34) Liu, X. J.; Moritomo, Y.; Nakamura, A.; Kojima, N. Pressure-Induced Phase Transition in Mixed-Valence Gold Complexes $Cs_2Au_2X_6$ (X=Cl and Br). *The Journal of Chemical Physics* **1999**, *110* (18), 9174–9178. https://doi.org/10.1063/1.478839.

(35) Momma, K.; Izumi, F. VESTA3 for Three-Dimensional Visualization of Crystal, Volumetric and Morphology Data. *Journal of Applied Crystallography* **2011**, *44* (6), 1272–1276. https://doi.org/10.1107/S0021889811038970.

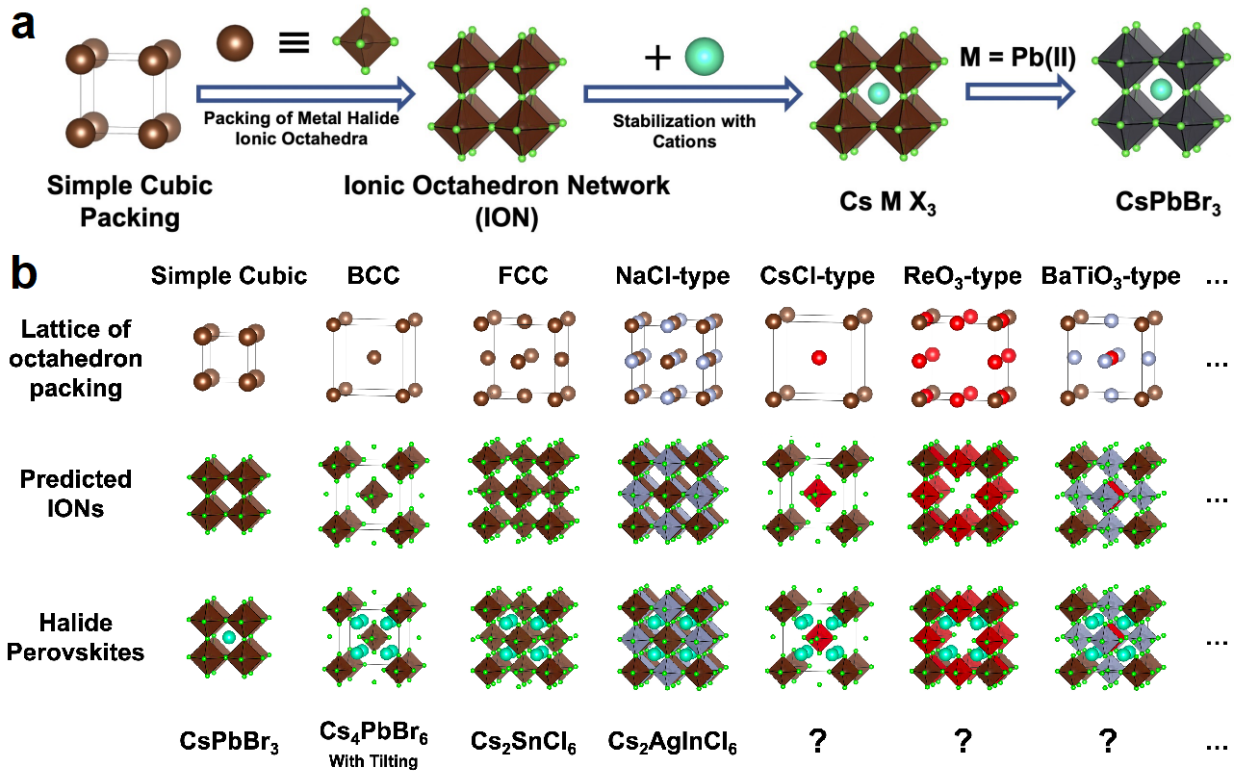

Scheme 1. Ionic Octahedron Network (ION). (a) Metal halide perovskites can be considered as extended Ionic Octahedron Networks (IONs) stabilized with positively charged cations. (b) Seven different lattices of octahedron packing and the predicted IONs and metal halide perovskite structures. Examples: The $CsPbBr_3$ halide perovskites can be considered as $[PbBr_6]$ octahedron placed in a simple cubic ION stabilized with Cs^+ cations; the vacancy ordered halide perovskite Cs_2SnCl_6 can be considered as the $[SnCl_6]$ octahedron placed in a face-centered cubic (FCC) ION stabilized with 8 Cs^+ cations. All of the crystal structures are plotted with VESTA software.[35]

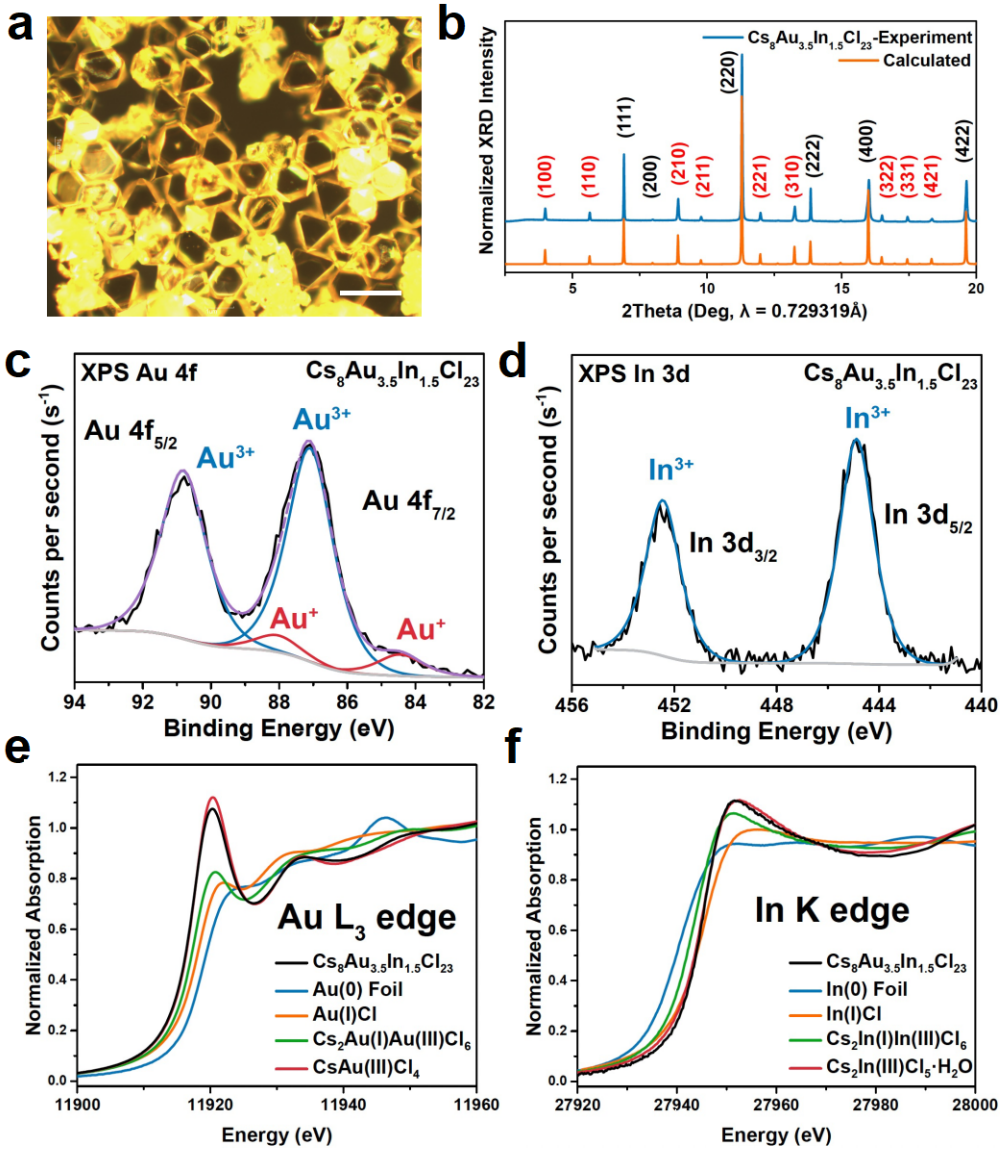

Figure 1. Characterization of $Cs_8Au_{3.5}In_{1.5}Cl_{23}$ crystals. (a) Optical microscope image (scale bar: 200 μm), (b) Experimental and calculated synchrotron powder x-ray diffraction patterns, (c, d) XPS on Au 4f and In 3d core level of $Cs_8Au_{3.5}In_{1.5}Cl_{23}$ crystals, respectively, XPS peaks for Au^{3+}, Au^{+} are labeled. (e, f) XANES on Au L_3 edge and In K edge of $Cs_8Au_{3.5}In_{1.5}Cl_{23}$ crystals, respectively. Au(0) foil, Au(I)Cl, $Cs_2Au(I)Au(III)Cl_6$ and $CsAu(III)Cl_4$ are used as reference samples for Au L_3-edge XANES, In(0) foil, In(I)Cl, $Cs_2In(I)In(III)Cl_6$ and $Cs_2In(III)Cl_5·H_2O$ are used as reference samples for In K-edge XANES,

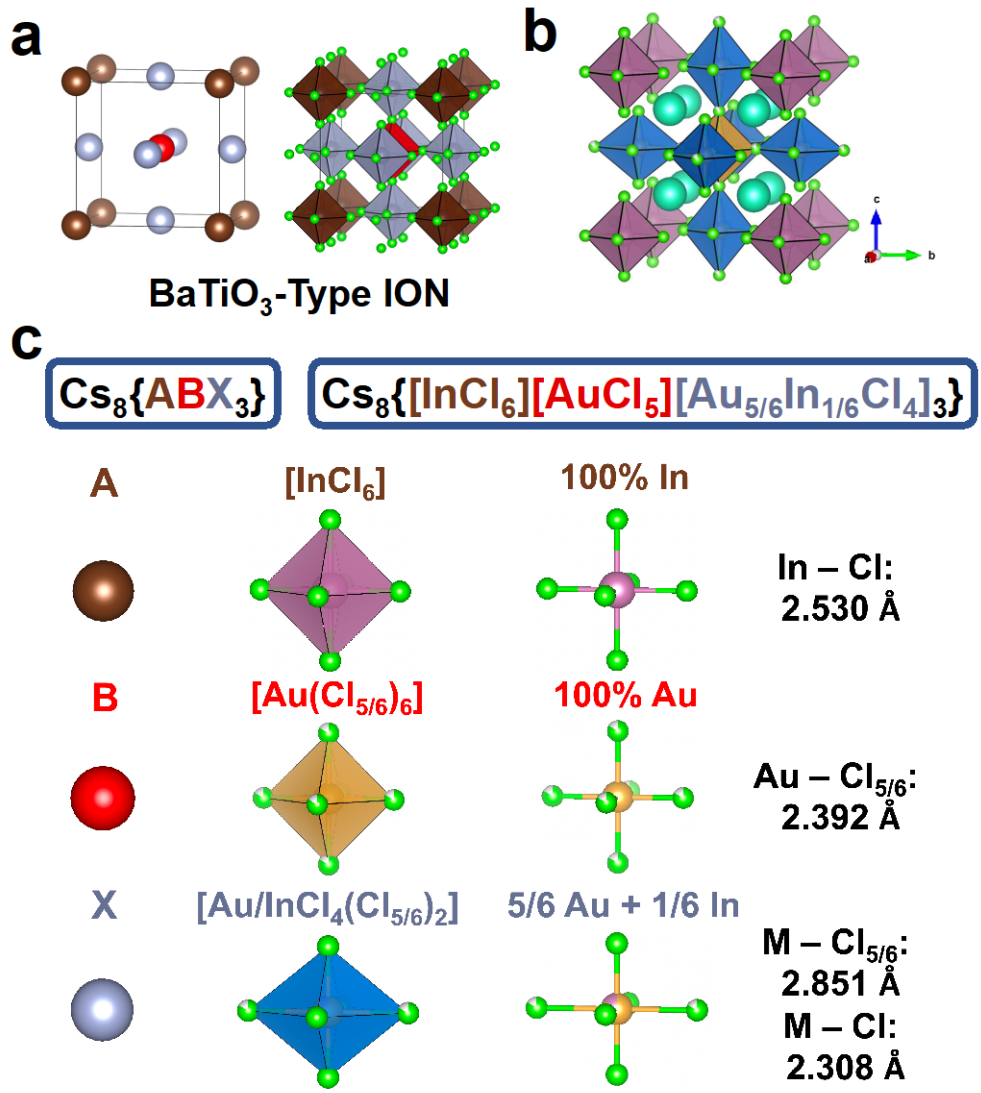

Figure 2. Single-crystal structure of $Cs_8Au_{3.5}In_{1.5}Cl_{23}$. (a) ION based on $BaTiO_3$ lattice packing, (b) View of the unit cell of $Cs_8Au_{3.5}In_{1.5}Cl_{23}$, (c) Each metal halide ionic octahedron and there representation in the ABX_3 based ION. (i) Super "A" site: Isotropic $[InCl_6]$ octahedron colored in purple; (ii) Super "B" site: $[Au(Cl_{5/6})_6]$ isotropic octahedron colored in yellow, centric Au atoms bonded with six bridging Cl atoms, which is only 5/6 occupied; (iii) Super "X" site is an elongated $[Au/InCl_4(Cl_{5/6})_2]$ octahedron colored in blue, the metal occupancy is 5/6 Au + 1/6 In.

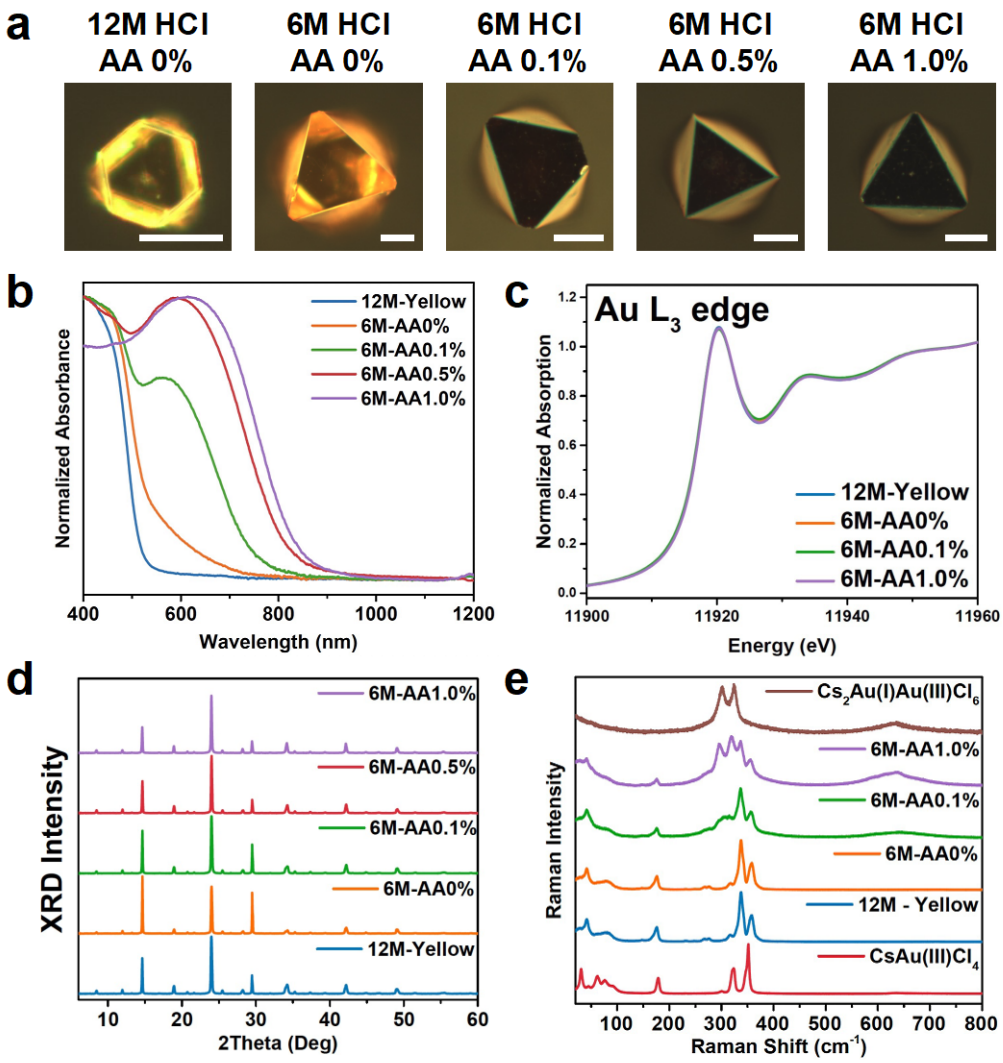

Figure 3. Au(I) induced bandgap narrowing in $Cs_8Au_{3.5}In_{1.5}Cl_{23}$ structure. (a) Optical microscope images (scale bar:100 μm), (b) UV-Vis-NIR absorption spectra, (c) XANES on Au L_3 edge, (d) powder XRD pattern, and (e) Low-frequency Raman spectra of $Cs_8Au_{3.5}In_{1.5}Cl_{23}$ crystals synthesized with different amounts of L-ascorbic acid (AA). $CsAu(III)Cl_4$ and $Cs_2Au(III)Au(III)Cl_6$ are used as reference samples in Raman experiments.

TABLE OF CONTENT